



Regular Article

Theoretical Prediction of the Size and Lifetime of Evaporating Sneeze Droplets in a Confined Space: A Guideline to Control of COVID-19 Virus Transmission

A. R. Bahramian *

Chemical Engineering Department, Hamedan University of Technology, P. O. Box: 65155, Hamedan, Iran

ARTICLE INFO

Article history:

Received: 2022-06-23

Accepted: 2023-01-28

Available online: 2023-01-29

Keywords:

Theoretical Evaporation Model, Indoor Environment, Sneeze Droplets, Size Distribution, Droplet Lifetime, COVID-19 Virus

ABSTRACT

The size and lifetime of evaporating sneeze droplets in the indoor environment were studied experimentally and theoretically. The effects of indoor temperature T_{∞} and indoor humidity RH_{∞} on evaporating droplets with the initial diameters of 4.9, 8.1, 17.2, and 29.7 μm were investigated. The size distribution and mean size of droplets were obtained by a laser particle sizer. The experimental data showed that the possibility of aerosolized droplets increased from 25.5 to 36.1 % by increasing T_{∞} from 18 to 30 $^{\circ}\text{C}$ and decreased from 36.1 to 13.6 % by increasing RH_{∞} from 30 to 60 %. A one-dimensional droplet evaporation model was used to estimate the lifetime of the droplet. A critical RH_{∞} of 40 % was found; above it, the lifetime of the droplet exponentially increases. The effect of the initial diameter of droplets was higher than that of RH_{∞} and also the impact of RH_{∞} was higher than that of T_{∞} on the lifetime of the aerosolized droplet nuclei. A significant effect of environmental conditions on the lifetime of the droplet was found over the range of $26\text{ }^{\circ}\text{C} \leq T_{\infty} \leq 30\text{ }^{\circ}\text{C}$ and $RH_{\infty} \leq 40\%$, while the effect decreased in the range of $18\text{ }^{\circ}\text{C} \leq T_{\infty} \leq 22\text{ }^{\circ}\text{C}$ and $RH_{\infty} > 40\%$, where a minimal shrinkage of droplets took place because of the hygroscopic growth of droplets. The results of this study do not imply that the COVID-19 virus will be deactivated at the end of the lifetime of the droplet, but it represents that controlling the indoor environment is important for droplets to carry the virus.

DOI: 10.22034/ijche.2023.348705.1447 URL: http://www.ijche.com/article_165980.html

1. Introduction

The COVID-19 disease, caused by the SARS-CoV-2 virus, has been detrimental to a billion

people around the globe [1]. The COVID-19 pandemic has provided an excellent demand for a better understanding of the spread of the

*Corresponding author: bahramian@hut.ac.ir (A. R. Bahramian)

virus in indoor environments. The SARS-CoV-2 virus can be transmitted by direct contact by exhaling virus-laden droplets or aerosols ejected from the expiratory activities of an infected person during coughing, sneezing, and even talking with a healthy person [2-4]. Face touching is a secondary transmission route of the SARS-CoV-2 virus [5], and another route is direct inhalation of virus-laden droplets or aerosolized droplet nuclei [6]. The World Health Organization (WHO) has reviewed available data to update guidelines for identifying the transmission routes and preventing the SARS-CoV-2 virus transmission [7]. To reduce the SARS-CoV-2 virus transmission, social distancing guidelines have been issued for confined spaces that require people to remain physically distant from each other at a distance of about two meters.

Based on the classification presented by the WHO, the respiratory droplets with diameters of smaller than 5 μm and larger than 100 μm are known as aerosolized droplet nuclei, and large droplets respectively. Saliva droplets with the diameters in the range of 5-100 μm are known as medium droplets. Liu et al. [8] identified that aerosols containing the SARS-CoV-2 virus are categorized in two groups with diameters in the ranges of 0.25-1.0 μm and $> 2.5 \mu\text{m}$. The saliva droplets with the diameters of larger than 100 μm tend to settle quickly on the ground because of gravity at distances less than one meter. In contrast, the droplets with smaller diameters than 50 μm evaporate into aerosolized droplet nuclei at distances of more than 1.5 m [9]. It is approved that the saliva droplets lose $\sim 20\text{-}38\%$ of their initial size due to the presence of nonvolatile compounds [10].

Earlier studies have confirmed that the viruses persist in the aerosolized droplet nuclei

with the ultimate diameter limit of $\sim 0.1\text{-}0.14 \mu\text{m}$, upon complete evaporation [11-13]. Li et al. [11] reported that the lifetime of the droplet depends on the initial diameter of the exhaled droplets. They reported that the lifetime of pure water droplets of 50 μm in diameter was ~ 4.5 s, while in the case of droplets of 100 μm in diameter is ~ 8.5 s. The results showed that the lifetime of droplets increases by decreasing their diameter and increasing the content of nonvolatile compounds. Li et al. [11] also found that the lifetime of droplets with the salt mass fraction of 6.5 % at 30 °C and the RH_∞ of 84 % was 12.5 s. The aerosolized droplet nuclei can stay in the air for long times and transfer the virus over long distances. The virus survival in the indoor environment is dependent on the indoor temperature T_∞ , and indoor relative humidity RH_∞ [14]. van Doremalen et al. [15] found that the SARS-CoV-2 remained viable in aerosols throughout three hours. Bououiba [16] showed that the interaction of virus-laden droplets with the turbulence in flow plays a vital role in the spread of the virus. Balachandar et al. [7] showed that the large sneeze droplets could break up into smaller droplets with a higher lifetime than the initial droplets.

At high T_∞ , and low RH_∞ , a droplet could evaporate and shrink, which affect its trajectory and airborne transmission. The initial size and size distribution of expiratory droplets can influence the dynamic trajectory of droplets. Therefore, the accurate measurements of droplets play a key role in studying the airborne transmission of virus-laden droplets and planning the infection control [17]. There are different techniques to analyze the size distribution of droplets in literatures [18-21]. Duguid [18] found that the size distribution of cough and sneeze droplets ranged between 1 and 2000 μm , while 95 % of

droplets were between 2 and 100 μm using the solid impaction technique. Edwards et al. [19] used an optical particle counter to determine the size of droplets, in the range of 0.15 to 0.19 μm , exhaled from the breathing activity. Chao et al. [20] found that the geometric mean diameter of cough and sneeze droplets ranged between 13.5 μm for coughing and 16.0 for sneezing in 11 healthy subjects, by using the interferometric Mie imaging technique. Han et al. [21] reported that the geometric mean diameter of sneeze droplets was 360.1 μm for a unimodal distribution (one peak) and 74.4 μm for a bimodal distribution (two peaks) with the geometric standard deviations of 1.5 and 1.7 respectively. The effects of evaporation significantly influence the size distribution of droplets that are exhaled into the indoor environment to reach the final equilibrium diameter of droplets. In addition to experimental studies on the evaporation of aerosolized droplets, the theoretical models are well formulated in literatures [22-26]. The non-volatile components such as pathogens and salt and reaction kinetics can affect the evaporation rate and lifetime of droplets and be effective in the case of saliva droplets, while in the case of sneeze droplets, it can be assumed that the liquid composition is near to pure water. Liu et al. [27] found that the effect of non-volatile components is very low (less than 3 %) in the case of sneeze droplets.

The evaporation model of droplets was coupled with the mass transfer between the droplets and gas phases, which led to an increase in the complexity of the transport of sneeze droplets. Although several studies on the effect of the environmental conditions on the transport of sneeze droplets were performed in literatures, but the mutual impact of T_∞ and RH_∞ is less understood. The objective of the current study is to examine the

size and lifetime of the evaporating sneeze droplets in the indoor environment. The impact of T_∞ in the range of 18-32 $^\circ\text{C}$ and RH_∞ in the range of 30-60 % on evaporating droplets with the initial diameters of 4.9, 8.1, 17.2, and 29.7 μm was studied experimentally and theoretically. T_∞ were selected based on the ASHRAE (2017) regulations for indoor spaces [28], while RH_∞ values were selected based on the U.S. standard building design regulations ($\text{RH}_\infty < 65$ % as per ASHRAE 2013b (ANSI/ASHRAE 2013) [29]. The size distribution and mean size of droplets were obtained by a laser particle sizer. A one-dimensional droplet evaporation model was applied to estimate the lifetime of the droplet. The theoretical model invokes the assumptions of an the ideal gas mixture, spherical symmetry, constant binary diffusion, no re-condensation on the droplet surface, and constant physical properties of droplets. The results of this study can help to update the health guidelines to control virus-carrying droplets in different indoor environments.

2. Experimental section

2.1. Human participants

Ten boy and girl students within the age range of 22-23 years old were selected to analyze the droplet size distribution while sneezing. Table 1 shows the characteristics of the 20 healthy human participants in the sneeze experiments in the fluid mechanics laboratory of Hamedan University of Technology during 30 working days. Before executing the experiments, all participants presented the negative PCR test result. All participants completed the written consent and ethics statement. In addition, all participants underwent fever thermographic tests at the beginning and end of the experiments. The body-mass index (BMI) of male participants was in the range of 23.1-

26.0, while in the case of female participants, it was in the range of 22.3-24.8. The use of pepper stimulants helped the participants to sneeze more easily. All tests were performed in the morning and two hours after breakfast to minimize the effect of the food on the density and viscosity of the sneeze droplets. Experiments were performed on one person individually in one day to avoid transmitting the possible virus from person to person.

Participants were not allowed to drink water or other drinks before the tests. All experiments were carried out on one person individually in one day. At the end of the experiments, the equipment and the floor were disinfected with an alcoholic solution. In addition, the air conditioning system was activated to eliminate possible airborne virus agent. More details on the experimental procedure are available elsewhere [30].

Table 1

The characteristics of the 20 healthy human participants.

Case No.	Age (years)	Sex (M/F)	Height (H) (m)	Weight (W) (kg)	Body-mass index (BMI=W/H ²)
1	22	M	1.68	65.3	23.1
2	22	M	1.69	67.2	23.6
3	22	M	1.70	69.5	24.0
4	22	M	1.71	71.8	24.6
5	22	M	1.72	74.2	25.1
6	23	M	1.73	74.1	24.8
7	23	M	1.73	74.8	25.0
8	23	M	1.73	76.1	25.4
9	23	M	1.72	74.9	25.3
10	23	M	1.70	75.2	26.0
11	22	F	1.63	59.4	22.3
12	22	F	1.64	60.4	22.5
13	22	F	1.65	60.9	22.4
14	22	F	1.65	62.3	22.9
15	22	F	1.66	63.8	23.1
16	22	F	1.65	65.1	23.9
17	23	F	1.66	66.4	24.0
18	23	F	1.66	67.3	24.4
19	23	F	1.65	67.0	24.6
20	23	F	1.66	68.4	24.8

2.2. Droplet size distribution analysis

A laser particle sizer system (Malvern Instruments Ltd, UK) was applied to analyze the droplet size distribution, in the range of 0.1 to 1000 μm , while sneezing in different indoor environments. Figure 1 shows the schematic image of the laser particle sizer system. The laser beam with a diameter of 0.012 m was

produced by a helium-neon laser transmitter and passed through the measurement zone. Forty-two optical sensors were installed in the receive module to analyze the light diffraction pattern. A scattering model was used to examine the light diffraction pattern. The size distribution of the sneeze droplets was recorded at every 0.4 ms. Thus, the sampling

frequency was set as 2.5 kHz to ensure the measurement were real-time data acquisition processes. The possible biases in the estimation of the size of evaporating droplets along the longitudinal distance between the laser particle sizer and the participant's mouth were estimated by repeating experiments at different times. T_{∞} values were adjusted at 18, 22, 26, and 30 °C, while RH_{∞} values were fixed at 30, 40, 50, and 60 %.

The number size distribution, which is defined as the ratio of the total number of droplets in the range of 0.1-1000 μm to the total number of all the sneeze droplets with any diameters, can be determined by the following:

$$P_{n,i} = \frac{N_i}{N} = \frac{P_{V,i} \cdot V (1/6 \pi D_i^3)^{-1}}{\sum_i P_{V,i} \cdot V (1/6 \pi D_i^3)^{-1}} = \frac{P_{V,i} D_i^{-3}}{\sum_i P_{V,i} D_i^{-3}} \quad (1)$$

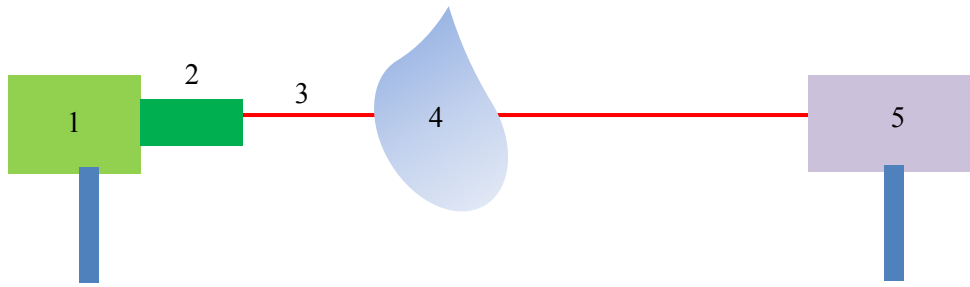


Figure 1. The schematic image of the laser particle sizer system, [1: Transmitter, 2: laser source, 3: laser beam, 4: sneeze droplets, 5: receiver].

3. Theoretical model

3.1. Droplet evaporation model

The evaporation rate of sneeze droplets is calculated by the mass transfer and species conservation equations of an evaporating droplet in the air.

Mass conservation equation:

$$\frac{d(r^2 \rho v)}{dr} = 0 \quad (2)$$

Species conservation equation:

$$\frac{1}{r^2} \frac{d(r^2 \rho v Y_w)}{dr} = \frac{1}{r^2} \frac{d}{dr} (r^2 \rho D \frac{dY_w}{dr}) \quad (3)$$

where v is the radial velocity, D is the binary

diffusivity coefficient, N is the total number of droplets, N_i is the total number of droplets in the diameter class i , where $i=1, 2, \dots, n$. $P_{n,i}$ is the droplet number fraction of droplets, $P_{V,i}$ is the ratio of the volume of all droplets with diameters in diameter class i to the total volume of all droplets with any diameter, V is the total volume of all droplets, and D_i is the mean diameter of droplets. According to our experiments, the mean total number of droplets ejected from participant's mouth is measured to be 5535 ± 43 , which corresponds to $5.535 \pm 0.043 \text{ \#/cm}^3$. The results were determined by averaging the data obtained from sneezing experiments through three repeated sneezes of each of participants.

diffusivity coefficient, and Y_w is the mole fraction of water vapor. The mass flux at the droplet surface can be calculated as:

$$\dot{m}_s = \rho_s D_s \frac{\ln(1+B_M)}{r_s} \quad (4)$$

where ρ_s is the density of the droplets at the surface, D_s is the binary diffusivity coefficient at the surface of the droplet, r_s is the radius of the droplet, and B_M is the Spalding mass transfer number [27]:

$$B_M = \frac{(Y_{w,s} - Y_{w,\infty})}{(1 - Y_{w,s})} \quad (5)$$

where, $Y_{w,s}$ and $Y_{w,\infty}$ are, respectively, the

mole fraction of the vapor at the surface of the droplet, and the mole fraction of the vapor at the dry air, which are calculated through the following relations:

$$Y_{w,s} = \frac{P_{vap}(T_s, X_{w,s}) M_w}{P_{vap}(T_s, X_{w,s}) M_w + (1 - P_{vap}(T_s, X_{w,s})) M_{da}} \quad (6)$$

$$Y_{w,\infty} = \frac{(RH_\infty) P_{sat}(T_\infty) M_w}{(RH_\infty) P_{sat}(T_\infty) M_w + (1 - (RH_\infty) P_{sat}(T_\infty)) M_{da}} \quad (7)$$

where $X_{w,s}$ is the mole fraction of water vapor and subscript da denotes the dry air. At $T_s > T_\infty$, it is expected that the droplets are cooled relatively to its initial temperature. At $T_s < T_\infty$, the heat is transferred from the air to the surface of an evaporating droplet until reaching the wet-bulb point. The lifetime of the droplet is obtained through solving the mass balance relationship of the droplet [27, 31]:

$$\frac{dm_f}{dt} = -4\pi r_s^2 \dot{m}_s \quad (8)$$

where subscript f denotes the water content inside the droplet. The lifetime of the droplet (t^*) is calculated by solving equation 8 with the initial boundary condition of $d_f(0) = d_0$,

$$t^* = \frac{\rho_f d_0^2}{8 \rho_w D_w (\ln(1+B_M))} \quad (9)$$

where d_0 is the initial diameter of droplets, and ρ_f and ρ_w are the densities of the liquid water and water respectively. d_0 corresponds to lifetime t^* of the droplet, which is defined as critical diameter d_{crit} . Both t^* and d_{crit} were dependent on the indoor environmental conditions (T_∞, RH_∞). d_0 was set based on the mean value of the droplet size distribution obtained from the laser particle sizer experiments. At an equilibrium diameter d_{eq} , the evaporation of the droplet is stopped. When $Y_{w,\infty}$ approximates to $Y_{w,s}$, B_M approaches zero, and t^* (Eq. 9) becomes infinit. Liu et al. [27] found that the droplet diameter follows

the d^2 -law:

$$d^2(t) = d_0^2 - k' t \quad (10)$$

where d_0^2 is the initial droplet diameter, and k' is the effective evaporation coefficient. Considering the dry and humid environments, the values of k' were reported to be 2.5×10^{-7} and $1.0 \times 10^{-9} \text{ m}^2 \cdot \text{s}^{-1}$ respectively [31]. The evaporation rate decreases to zero as the droplet approaches its equilibrium diameter $d_{eq} = d_0 \psi_0^{1/3}$, where ψ_0 is the volume fraction of the non-volatile component in the droplet at the time of ejection, which is taken to be 2 % [32]. The coupled equations (Eq. 2 and 3) are solved numerically by MATLAB codes using the forth-order Range-Kutta method.

3.2. Boundary conditions and assumptions

The main boundary conditions used in the mathematical model are:

$$r = r_s \quad \rho_s v_s = \rho_s v_s Y_w + (-\rho D) \left(\frac{dY_w}{dr} \right)_s \quad (11)$$

$$r \rightarrow \infty \quad Y_w = Y_{w,\infty} \quad (12)$$

The main assumptions used in the mathematical model are:

1. the carrier gas (indoor air) is treated as an ideal gas.
2. A one-dimensional transport in r-direction (spherical symmetry) is considered in the model by assuming the quasi-steady state condition.
3. No re-condensation is considered on the droplet surface, while the binary diffusion of the water vapor from the droplet surface to indoor air is considered in the equation.
4. The binary diffusivity coefficient, D , at the droplet surface and the $\rho v r^2$ term are assumed to be constant in Equation 3.

5. Only 5 % of the mass fraction of sneeze droplets is assumed to contain non-volatile compounds based on literatures [20].

6. the constant thermodynamic properties of

the sneeze droplets (i.e. density, mole fraction) are assumed in the mathematical model. Table 2 shows the thermodynamic and transport property values used in computing the lifetime of the droplet.

Table 2

The thermodynamic and transport property values used in computing the lifetime of the droplet.

T_{∞} (°C)	ρ_f (kg/m ³)	ρ_w (kg/m ³)	$P_{w,sat}$ (atm)	D_v (m ² /s)
18	9.979×10^2	1.729×10^{-2}	1.947×10^{-2}	2.418×10^{-2}
22	9.979×10^2	1.729×10^{-2}	2.680×10^{-2}	2.418×10^{-2}
26	9.979×10^2	1.729×10^{-2}	3.413×10^{-2}	2.418×10^{-2}
30	9.979×10^2	1.729×10^{-2}	4.146×10^{-2}	2.418×10^{-2}

4. Results and discussion

Figure 2 shows the size distribution of droplets at the (a) T_{∞} of 18, 22, 26, and 30 °C and $RH_{\infty} = 30$ % and (b) RH_{∞} of 30, 40, 50, and 60 % and $T_{\infty} = 18$ °C. The results were obtained by the laser particle sizer system at 0.5 s after sneezing. The mean diameter of the droplets varied from 29.7 to 4.9 μm according to the changes in the T_{∞} (Figure 2a) and RH_{∞} (Figure 2b). The number of aerosolized droplet nuclei was increased by increasing T_{∞} and decreasing RH_{∞} . The mean diameter of the droplets decreased from 8.1 ± 0.5 to 4.9 ± 0.4 μm by increasing the T_{∞} from 18 to 30 °C at $RH_{\infty} = 30$ % (Figure 2a), while its value increased from 17.2 ± 0.8 to 29.7 ± 1.0 μm by increasing the RH_{∞} from 30 to 60 % at $T_{\infty} = 18$ °C (Figure 2b). These results indicate the effect of RH_{∞} on the size distribution of droplets being higher than the T_{∞} . The continuous changes in the aerodynamic diameter of the droplets are an important reason for the inaccuracy of the results, especially at high RH_{∞} values, which was mentioned in literatures [20, 26, 27].

The number of aerosolized droplet nuclei increased from 25.5 to 36.1 % by increasing T_{∞} from 18 to 30 °C at $RH_{\infty} = 30$ %, while the

number of aerosols decreased from 36.1 to 13.6 % by increasing the RH_{∞} from 30 to 60 % at $T_{\infty} = 30$ °C. In addition, the number of medium droplets increased from 41.4 to 50.6 % by increasing T_{∞} from 18 to 30 °C at $RH_{\infty} = 30$ % (Figure 2a), while the number of large droplets decreased by increasing T_{∞} . The effect of RH_{∞} on the diameter and number of large droplets was negligible (Figure 2b). The data analysis shows an increase of RH_{∞} from 30 to 60 % resulting in a slight increase (~ 8 %) in the number of large droplets. Morawska et al. [32] found that the hygroscopic growth of the droplets was most influenced by RH_{∞} . In contrast, the evaporation rate was most influenced by T_{∞} . Therefore, the impact of RH_{∞} was considerably higher than the effect of T_{∞} on the reduction of the number and diameter of aerosolized droplet nuclei and medium droplets. The effect of T_{∞} was significantly higher than the effect of RH_{∞} on the decrease in the number and diameter of large droplets. These results indicate that the persistence of the virus agent in the air can substantially affect the infection agent's controlling strategy.

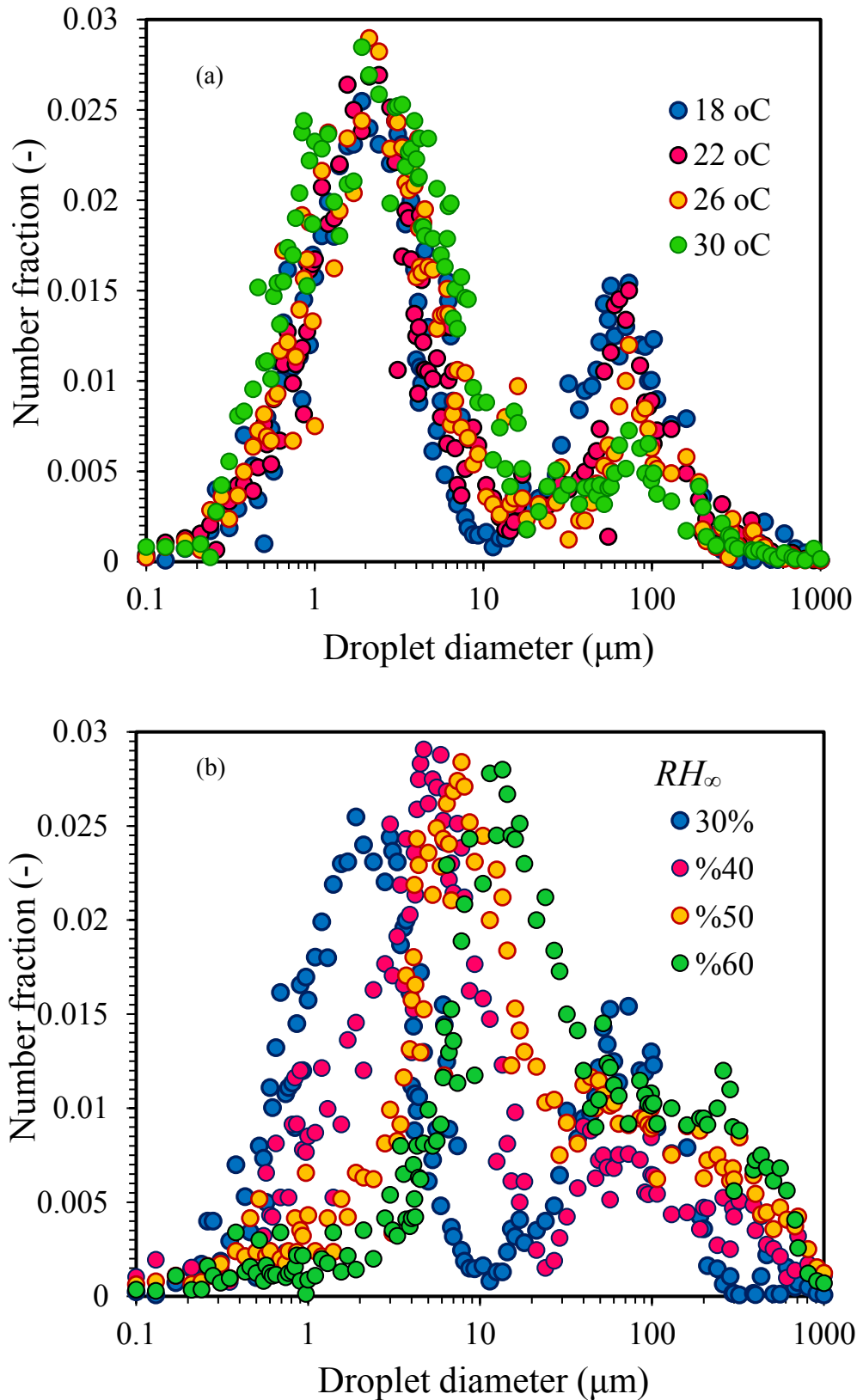


Figure 2. The size distribution of droplets at the (a) T_{∞} of 18, 22, 26, and 30 °C at $RH_{\infty} = 30\%$ and (b) RH_{∞} of 30, 40, 50, and 60 % and $T_{\infty} = 18\text{ }^{\circ}\text{C}$ [the results were obtained at 0.5 s after sneezing].

Figure 3 shows the variation of the normalized square of the diameter of the

droplet (d_{eq}/d_0)² the versus evaporation time at different mean diameters, and the T_{∞} of 18 (a),

22 (b), 26 (c), and 30 °C (d). The mean diameters of 4.9, 8.1, 17.2, and 29.7 μm were selected in the theoretical model based on the mean diameters of droplets obtained from experiments, while RH_∞ was set to 40 %. It can be seen that $(d_{\text{eq}}/d_0)^2$ varies linearly with the evaporation time following the d^2 -law of Spalding. Also, the results showed that the $(d_{\text{eq}}/d_0)^2$ significantly decreases by decreasing the initial diameter and it also slightly decreases by increasing T_∞ . This result indicates that the evaporation time depends significantly on the initial diameter of the droplet. The large droplets require a higher time to evaporate than the smaller ones due to their large volume to surface area ratio. For example, a 4.9 μm droplet evaporates in 2.9 s, whereas a 29.7 μm droplet evaporates in 11.1 s at 18 °C (Figure 3a). The diameter of aerosolized droplet nuclei are between 23 to 31 % of the initial diameter of the droplet, depending to d_0 and T_∞ , as indicated by the horizontal lines, which were consistent with the reported results in literatures [11, 20, 27]. In the same droplet diameter of 4.9 μm , the droplet evaporates in 2.6, 2.2, and 1.9 s at 22 °C (Figure 3b), 26 °C (Figure 3c), and 30 °C (Figure 3d) respectively. In contrast, at the same droplet diameter of 29.7 μm the droplet evaporates at 10.2, 9.8, and 8.6 s at 22 °C (Figure 3b), 26 °C (Figure 3c), and 30 °C (Figure 3d) respectively. Therefore, the effect of d_0 on evaporation time was higher than that of T_∞ under the studied conditions.

The minimum and maximum effect of T_∞ on the evaporation time were found at 18 °C (Figure 3a) and 30 °C (Figure 3d), which indicate that the evaporation time significantly decreases by increasing T_∞ . Jafari et al. [33] found that by increasing T_∞ , the steady-state temperature of the droplet increased and droplet faster reached the wet-bulb

temperature. The equilibrium diameter of the droplet decreases by increasing T_∞ from 18 to 30 °C. At the T_∞ of 18 and 30 °C, the equilibrium droplet lies in the range of 25-31 %, and 23-25 % of the initial diameter of the droplet respectively. An increase in the initial diameter of droplet from 4.9 to 29.7 μm led to an increase in the ratio of the equilibrium diameter of the droplet to the initial diameter of the droplet from 4.9 to 29.7 μm ($d_{\text{eq},4.9 \mu\text{m}} / d_{\text{eq},29.7 \mu\text{m}}$), and this trend gets growing by increasing T_∞ . The rise in T_∞ from 18 to 22, 26, and 30 °C led to the increase in the ratio of $d_{\text{eq},29.7 \mu\text{m}} / d_{\text{eq},4.9 \mu\text{m}}$, from 22.3 to 25.9, 28.3, and 30.2 % respectively. This result indicates that the effect of the initial diameter of droplets was higher than that of T_∞ on the aerosolized droplet nuclei.

Figure 4 shows the variation of the normalized square of the diameter of the droplet $(d_{\text{eq}}/d_0)^2$ the versus evaporation time at different initial diameters, and the RH_∞ of 30 (a), 40 (b), 50 (c), and 60 % (d). T_∞ was set to 22 °C. The results show a decrease of $(d_{\text{eq}}/d_0)^2$ by increasing the evaporation time of droplets which follows the similar trend that was seen in the previous findings. As the diameter of droplets increases by increasing RH_∞ , thus the lifetime of droplets significantly increases by increasing RH_∞ . The results also showed that the evaporation time and aerosolized droplet nuclei depend greatly on the initial diameter of the droplet and RH_∞ . At the $\text{RH}_\infty = 30 \%$ (Figure 4a), a 4.9 μm droplet evaporates in 2.8 s, while a droplet with the diameter of 50 μm evaporates in 7.6 s at $\text{RH}_\infty = 60 \%$ (Figure 4a). This result indicates that an increase of two times in RH_∞ led to an increase of 2.7 times in the evaporation time of the droplets. In addition, the droplet nuclei are between 21 to 34 % of the initial diameter of the droplet, which indicates that the effect of the initial

diameter of droplets on the equilibrium diameter of the droplet was higher than that of RH_{∞} . In the same droplet diameter of $4.9 \mu\text{m}$, the droplet evaporates in 2.9, 3.2, and 3.5 s at 40 (Figure 4b), 50 (Figure 4c), and 60 % (Figure 4d) respectively. In contrast, at the

same droplet diameter of $29.7 \mu\text{m}$ the droplet evaporates in 9.7, 10.2, and 10.5 s at 40 (Figure 4b), 50 (Figure 4c), and 60 % (Figure 4d) respectively. Therefore, the effect of the initial diameter on the evaporation time was higher than that of RH_{∞} .

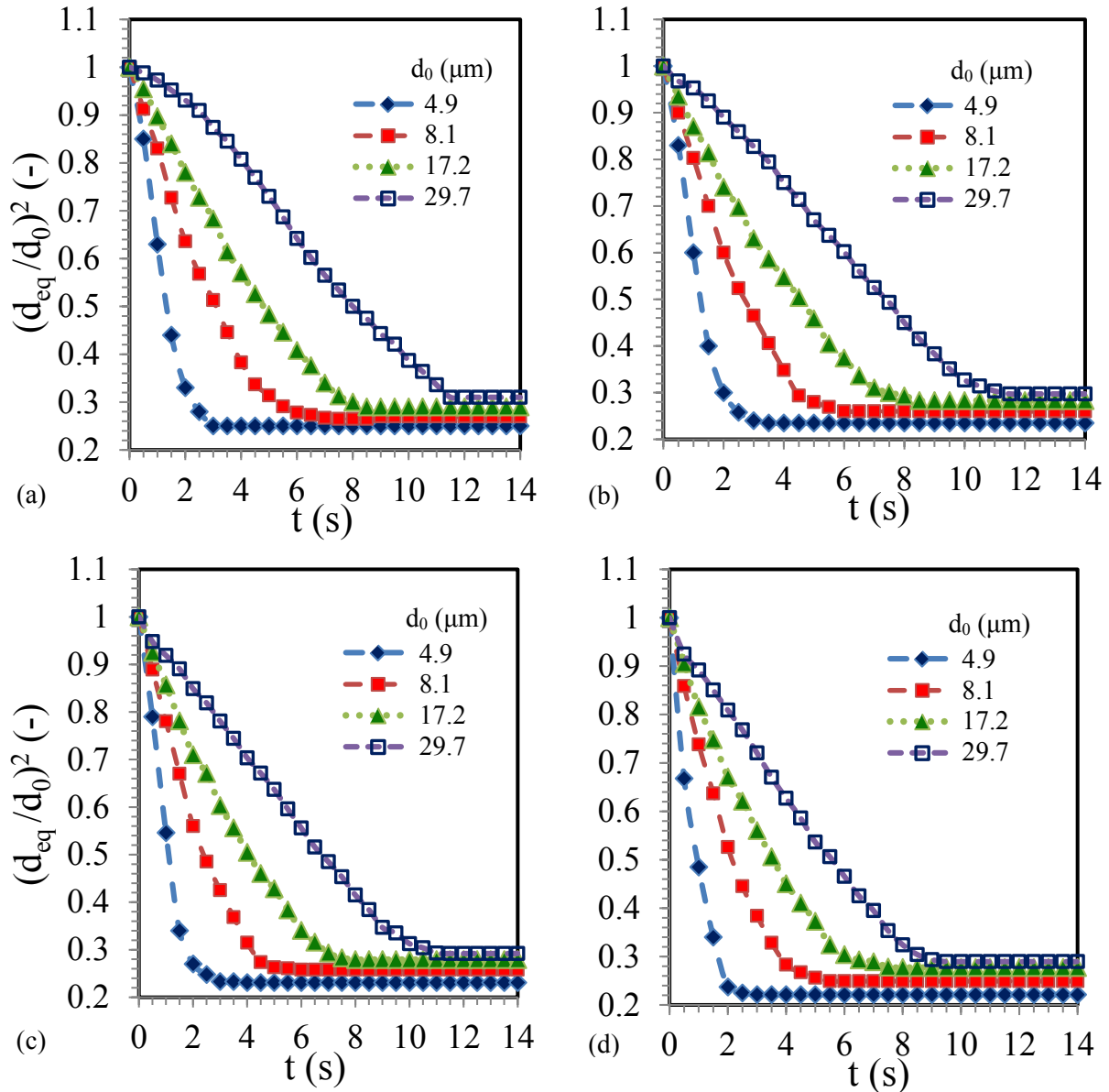


Figure 3. The variation of the normalized square of the droplet diameter $(d_{eq}/d_0)^2$ versus the evaporation time at different d_0 , $RH_{\infty} = 40 \%$, and T_{∞} of 18 (a), 22 (b), 26 (c), and 30 °C (d).

The minimum and maximum effect of RH_{∞} on the evaporation time of the normalized square of the diameter of the droplet $(d/d_0)^2$ was found, respectively, at 30 % (Figure 4a) and 60 % (Figure 4d). In addition, the

aerosolized droplet nuclei lie in the range of 21-24 %, and 29-34 % of the initial diameter of the droplet at the RH_{∞} of 30 and 60 % respectively. This result indicates that the effect of RH_{∞} was higher on the diameter of

droplet nuclei than on the initial diameter. The increase in RH_∞ from 30 to 40, 50, and 60 % led to the increase in the ratio of $d_{eq,29.7 \mu m} / d_{eq,4.9 \mu m}$, from 29.2, 25.9, 13.6, and 5.8 %

respectively. This finding confirms the effect of RH_∞ on the final diameter of droplet nuclei is higher than that of T_∞ .

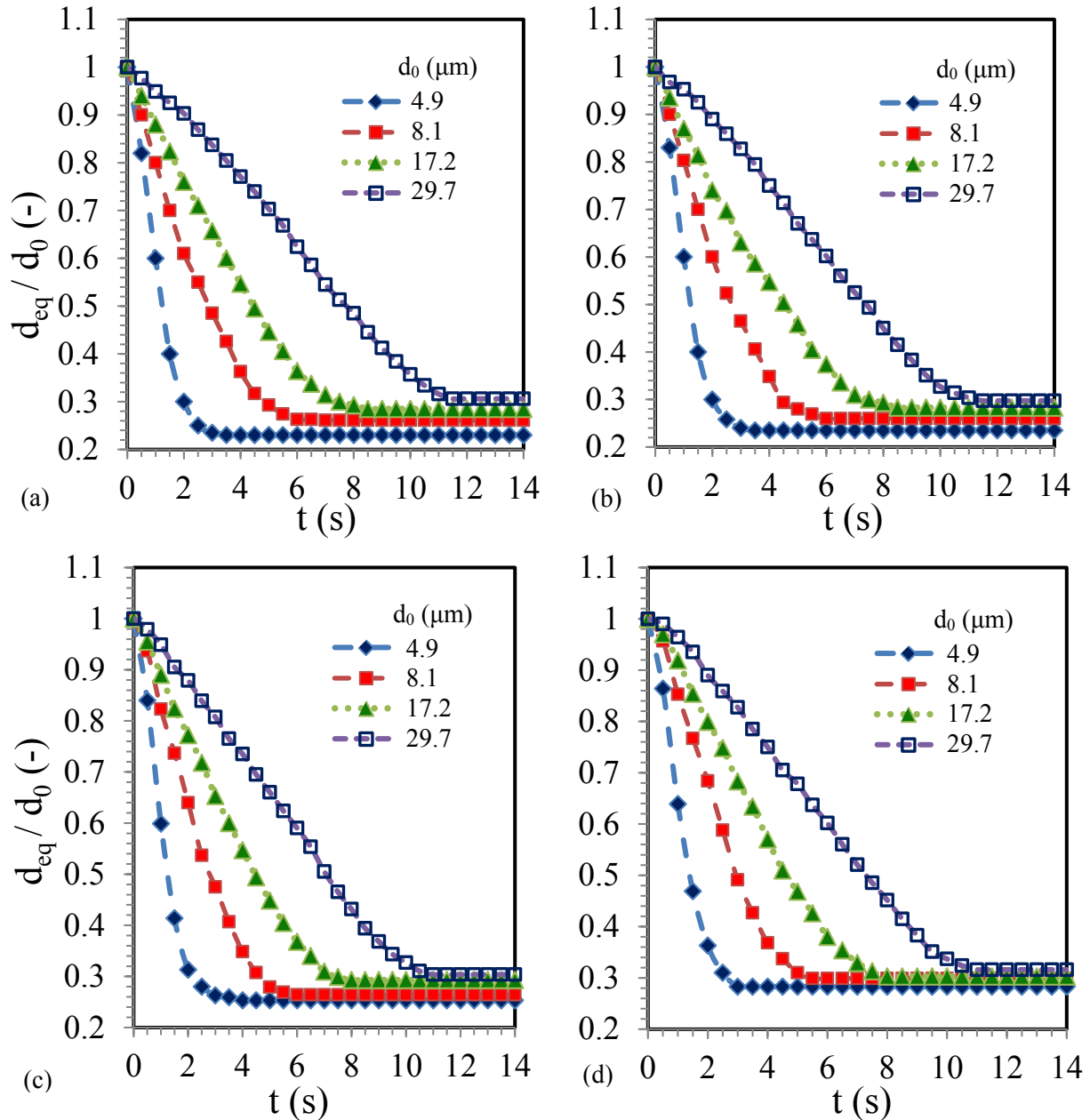


Figure 4. The variation of the normalized square of the droplet diameter $(d/d_0)^2$ versus the evaporation time at different d_0 , $T_\infty = 22$ °C, and RH_∞ of 30 (a), 40 (b), 50 (c), and 60 % (d).

Figure 5 shows the time evolution of the total mass normalized by the initial mass of droplets (m_s/m_0 ratio) at different initial diameters and the T_∞ of 18 (a), 22 (b), 26 (c), and 30 °C (d) and $RH_\infty = 40$ %. The results show that the m_s/m_0 ratio decreases considerably by

increasing the evaporation time due to the evaporation of droplets and then reach to a constant value, where the evaporation of droplets is typically stopped because of the existence of non-volatile compounds that are considered in the mathematical model. This

result indicates that the evaporation of tiny droplets affects the small droplets less than a few seconds after the emission. This result agreed with reported data for sneeze droplets [8, 28, 33]. Morawska et al. [32] showed that the sneeze droplets in the range of 1 to 10 μm exist for up to a few milliseconds to a few tens of seconds, while the droplets more than 100 μm can remain in the air up to several minutes. As it's clearly seen, the total mass of the

droplets was significantly decreased by increasing T_∞ . Obviously, a 29.7 μm droplet requires a higher time than a 4.9 μm droplet to evaporate. At $T_\infty = 18^\circ\text{C}$, the ratio of m_s/m_0 reaches the equilibrium mass of the droplet within 5.5 s, while in the case of a 29.7 μm droplet it occurs within 12.0 s (Figure 5a). The results show the increase of T_∞ from 18 to 22, 26, and 30 $^\circ\text{C}$, led to the decrease of 6.2, 7.8, and 9.6 % in the m_s/m_0 ratio respectively.

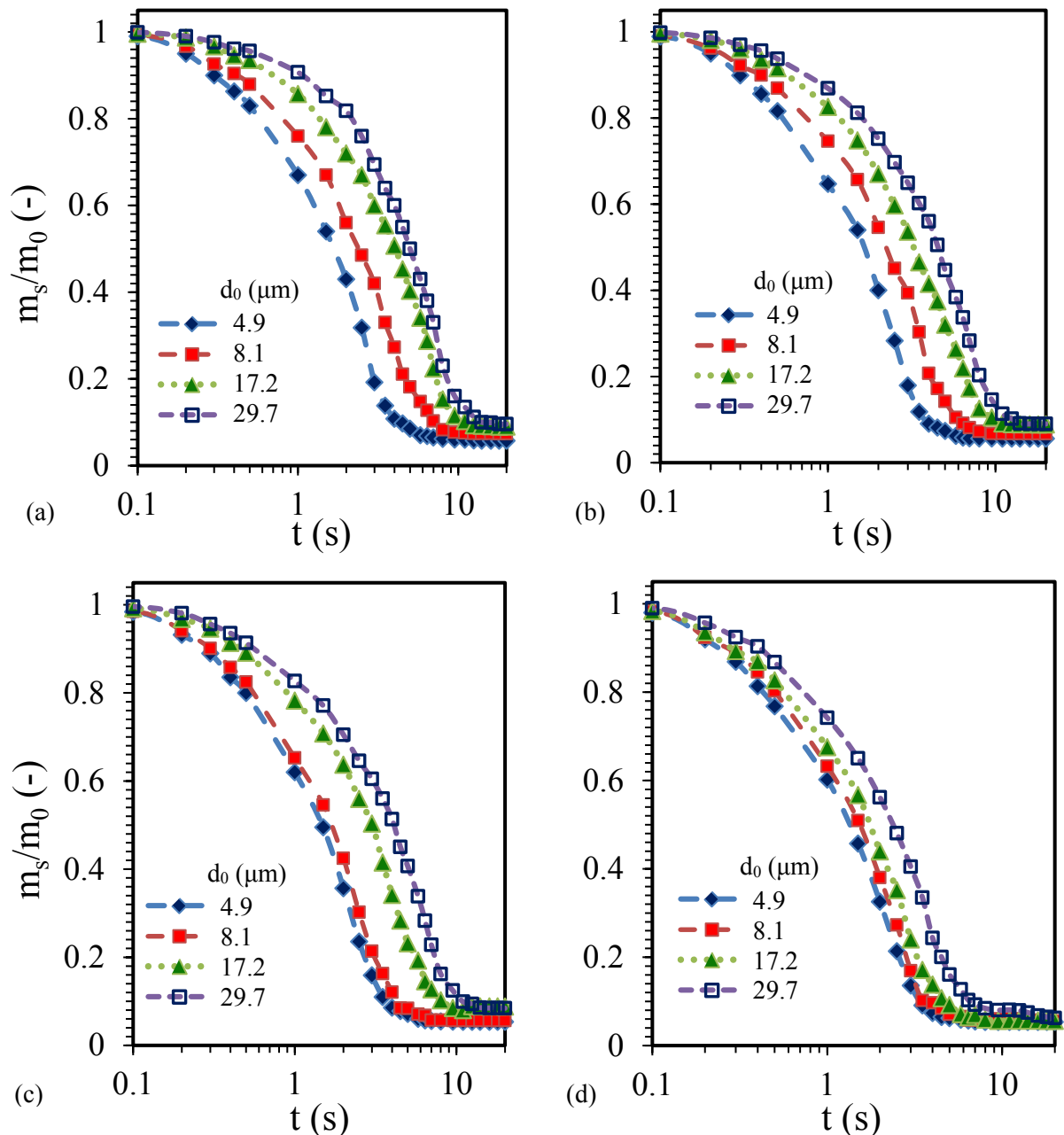


Figure 5. The time evolution of the total mass normalized by the initial mass of droplets (m_s/m_0) at different initial diameters and the T_∞ of 18 (a), 22 (b), 26 (c), and 30 $^\circ\text{C}$ (d) and $\text{RH}_\infty = 30\%$.

At $T_{\infty} = 18\text{ }^{\circ}\text{C}$ (Figure 5a), the rise of initial diameter from 4.9 to 8.1, 17.2, and 29.7 μm led to the increase of 12.8, 18.6, and 30.7 % in the m_s/m_0 ratio respectively. A similar result was found by applying the T_{∞} of 22 $^{\circ}\text{C}$ (Figure 5b), which indicates that the effect of the initial diameter was higher than the T_{∞} on the variations of the m_s/m_0 ratio. At $T_{\infty} = 26\text{ }^{\circ}\text{C}$ (Figure 5c), the effect of T_{∞} on the m_s/m_0 ratio and the time of the equilibrium mass of the droplet is minor in the case of 4.9 and 8.1 μm droplets, while its effect becomes more prominent in the case of 17.2 and 29.7 μm droplets. At $T_{\infty} = 30\text{ }^{\circ}\text{C}$ (Figure 5d), the effect of T_{∞} on the m_s/m_0 ratio and the time of the equilibrium mass of the droplet is negligible in the case of 4.9 to 17.2 μm droplets, while in the case of 29.7 μm droplets it led to a decrease in the m_s/m_0 ratio, which indicates the effect of the initial diameter of the droplet on the m_s/m_0 ratio significantly decrease by the increase of T_{∞} . In addition, the minimum and maximum effect of T_{∞} on the m_s/m_0 ratio were found at 18 $^{\circ}\text{C}$ (Figure 5a) and 30 $^{\circ}\text{C}$ (Figure 5d), which indicates that the m_s/m_0 ratio significantly decreases by increasing the T_{∞} .

Figure 6 shows the time evolution of the total mass normalized by the initial mass of droplets (m_s/m_0) at different initial diameters at the RH_{∞} of 30 (a), 40 (b), 50 (c), and 60 % (d) and $T_{\infty} = 18\text{ }^{\circ}\text{C}$. The ratio of m_s/m_0 decreases by increasing the evaporation time, and its value increases by increasing RH_{∞} . At $\text{RH}_{\infty} = 30\text{ }%$ (Figure 6a), a droplet with a 29.7 μm diameter requires a significantly lower evaporation time than the droplet with an 8.1 μm diameter at $\text{RH}_{\infty} = 60\text{ }%$ (Figure 6d), which indicates that the effect of the initial diameter of the droplet on the evaporation of droplets was higher than that of RH_{∞} . At the $\text{RH}_{\infty} = 30\text{ }%$, the m_s/m_0 ratio of the droplet with a 4.9 μm diameter reaches to the equilibrium mass within 2.6 s,

while in the case of a 29.7 μm droplet it occurs within 10.9 s (Figure 6d). Also, the increase of RH_{∞} from 30 to, 40, 50, and 60 % led to the decrease of 10.1, 21.4, and 33.6 % in the m_s/m_0 ratio respectively. At the $\text{RH}_{\infty} = 30\text{ }%$ (Figure 6a), the rise in the initial diameter of droplets from 4.9 to 8.1, 17.2, and 29.7 μm , led to the increase of 10.2, 15.7, and 20.4 % in their m_s/m_0 ratio respectively. At the $\text{RH}_{\infty} = 50\text{ }%$ (Figure 6c), the impact of RH_{∞} on the m_s/m_0 ratio is minor in the case of 4.9 μm droplets, while an increasing trend in the m_s/m_0 ratio was found in the case of 8.1 to 29.7 μm droplets. At the $\text{RH}_{\infty} = 60\text{ }%$ (Figure 6d), the m_s/m_0 ratio of all droplets was influenced by RH_{∞} , which confirms that the effect of RH_{∞} was higher on the m_s/m_0 ratio than on the initial diameter of the droplet. Thus, a critical RH_{∞} value of 60 % was found, where all sneeze droplets affect the environmental conditions. These results were consistent with the available data in literatures [8, 27, 29, 34]. Liu et al. [27] reported that the risk of COVID-19 transmission was inversely proportional to RH_{∞} . They found that the virus viability was reduced at RH_{∞} by more than 57 % because of the restrictions on the evaporation rate of virus-laden droplets.

Figure 7 shows the distribution of d_{crit} (a) and t^* (b) over the T_{∞} values of 18 to 30 $^{\circ}\text{C}$ and RH_{∞} of 30 to 60 %. Generally, the droplets with $d_0 \neq d_{\text{crit}}$ can transmit the virus, while the droplets with $d_0 = d_{\text{crit}}$ evaporate or settle before the airborne transmission (Figure 7a). In the case of droplets with $d_0 < d_{\text{crit}}$ the evaporation process takes place, while droplets with $d_0 > d_{\text{crit}}$ settle on the ground due to gravity. At highest studied T_{∞} (30 $^{\circ}\text{C}$) and lowest RH_{∞} (30 %), the droplets shrink due to the high evaporation rate before they can settle, while at the lowest T_{∞} and highest RH_{∞} , the smaller droplets cannot quickly evaporate and

remain in the air for long times. A small value of d_{crit} was obtained at the lowest T_{∞} (18 °C) and highest RH_{∞} (60 %), while a significant value of d_{crit} was obtained at the highest T_{∞} and lowest RH_{∞} (Figure 7a). The evaporation time of the droplets with diameter d_{crit} , which was mentioned as the droplet lifetime t^* is shown in Figure 7b. Despite the different initial diameters of droplets, t^* reaches its minimum value at the highest T_{∞} and lowest RH_{∞} , while

t^* reaches its maximum value at the lowest T_{∞} and highest RH_{∞} . Balusamy et al. [34] found that the longest lifetime of droplets was observed with the combination of a low T and high RH. An increase in the diameter of droplets led to reductions in the lifetime of droplets, where the aerosolized droplet nuclei can remain suspended under the dry indoor condition for longer times than the medium and large droplets.

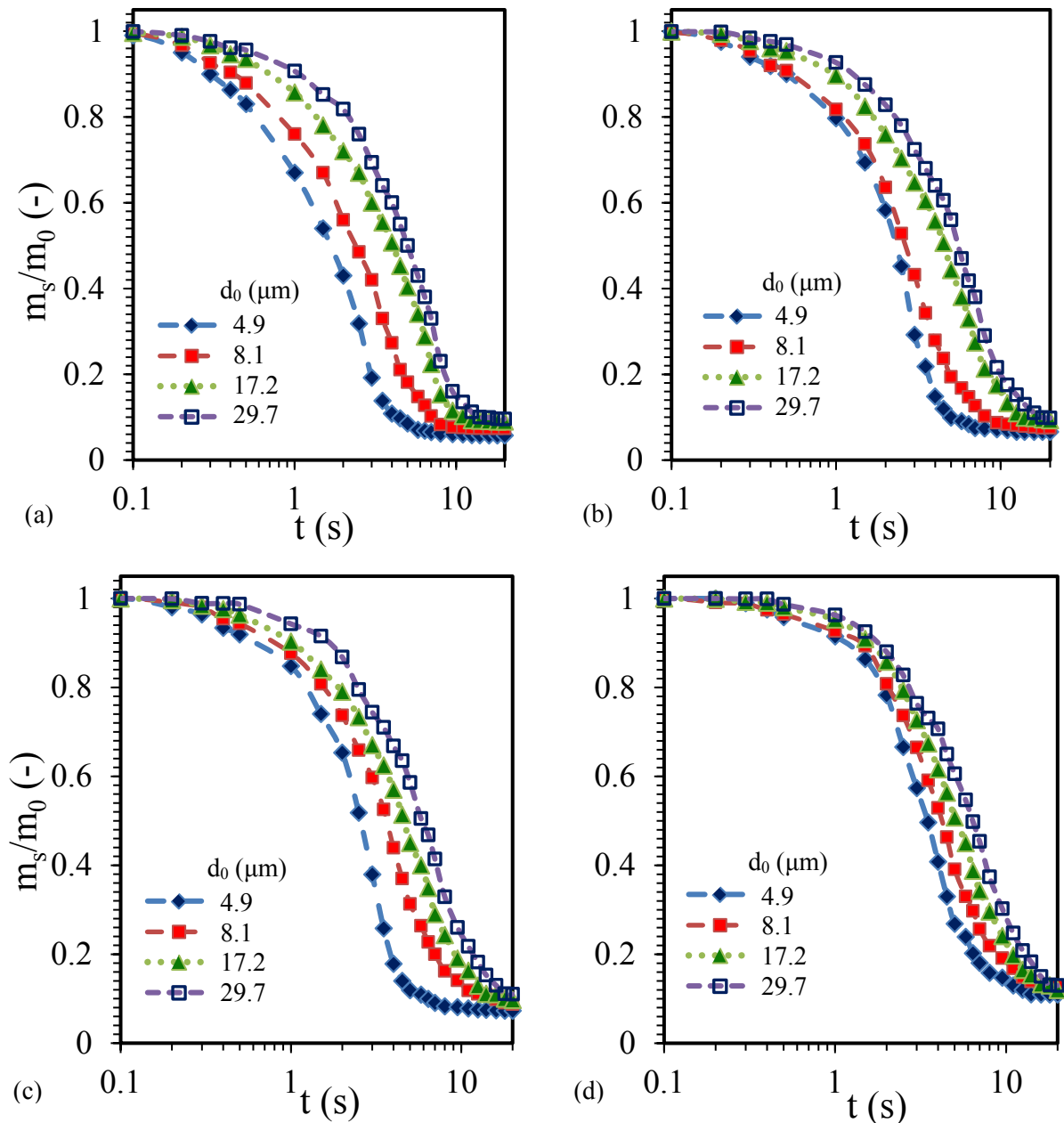


Figure 6. The time evolution of the total mass normalized by the initial mass of droplets (m_s/m_0) at different initial diameters at the T_{∞} of 18 °C, and RH_{∞} of 30 (a), 40 (b), 50 (c), and 60 % (d).

At the $RH_{\infty} \geq 50\%$ and $18\text{ }^{\circ}\text{C} \leq T_{\infty} \leq 22\text{ }^{\circ}\text{C}$, corresponding to a humid and moderate environment, the contour lines for all droplets with the same initial diameter were straightened, which indicates that the effect of RH_{∞} was higher than that of the initial droplet diameter. At the $RH_{\infty} \leq 40\%$ and $26\text{ }^{\circ}\text{C} \leq T_{\infty} \leq 30\text{ }^{\circ}\text{C}$, corresponding to a dry and warm environment, the contour lines tend to bend in the case of droplets with different initial diameters, which represents the lifetime of the droplet decreasing due to the high evaporation rate of the droplets. The results indicate that

the small droplets evaporate faster and shrink more in d_{crit} than the large droplets. In a warm and dry environment, the effect of the initial diameter of the droplet on the lifetime of the droplet was higher than that of RH_{∞} , and also the impact of RH_{∞} was higher than that of T_{∞} . Under humid and moderate environmental conditions, the effect of RH_{∞} on the lifetime of the droplet was higher for the the initial droplet. Therefore, it can be concluded that the RH_{∞} controlling a confined space plays a more influential role than T_{∞} in the survival of the virus agent in a confined space.

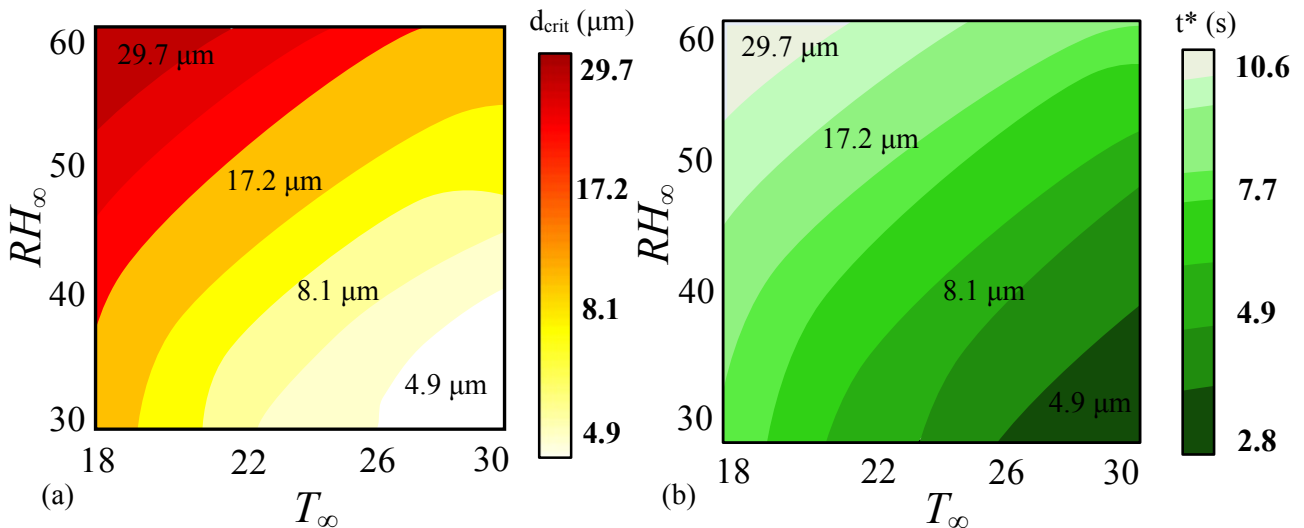


Figure 7. The distribution of d_{crit} (a) and t^* (b) over the T_{∞} of 18-30 $^{\circ}\text{C}$ and RH_{∞} of 30 to 60 % according to the standard indoor environment in the confined spaces.

Figure 8 shows the calculated results of the lifetime of the droplet (t^*) in second (s) versus RH_{∞} (%) at different T_{∞} values for different initial diameters of droplets (d_0). The results indicate that the lifetime of the droplet increases by increasing RH_{∞} and it increases by increasing the initial diameter of the droplet as indicated in Eq. 10 ($t^* \propto d_0^2$). The results show that an increase in T_{∞} does not necessarily lead to a decrease in the lifetime of the droplet, which confirms the effect of RH_{∞} on the lifetime of the droplet was higher than the impact of T_{∞} . At the $RH_{\infty} \geq 50\%$ and

$18\text{ }^{\circ}\text{C} \leq T_{\infty} \leq 22\text{ }^{\circ}\text{C}$, the effect of RH_{∞} was higher than that of T_{∞} , while the effect of T_{∞} on the lifetime of the droplet became more influenced due to the high evaporation rate of the droplets over the range of $26\text{ }^{\circ}\text{C} \leq T_{\infty} \leq 30\text{ }^{\circ}\text{C}$ and $RH_{\infty} \leq 40\%$. Thus, a higher T_{∞} and lower RH_{∞} can decrease the lifetime of the droplet. In addition, the results show that the initial diameter of the droplet has a significant effect on the lifetime of droplets at the $RH_{\infty} \leq 40\%$ and $26\text{ }^{\circ}\text{C} \leq T_{\infty} \leq 30\text{ }^{\circ}\text{C}$, while its effect decreases over the range of $18\text{ }^{\circ}\text{C} \leq T_{\infty} \leq 22\text{ }^{\circ}\text{C}$ and $RH_{\infty} \geq 50\%$, where a minimal shrinkage

of droplets takes place because of the hygroscopic growth of the droplets. The obtained result is in good agreement with the data reported by Katre et al. [35], which indicates that in a low T_∞ and humid environment, a droplet cloud takes longer to evaporate, and its lifetime decreases as the humidity decreases and temperature increases. They found that the respiratory droplet cloud loses over 60 % of its initial liquid mass during 5 s [35]. The calculated lifetime of the droplet increased from 2.8 s (at $RH_\infty = 30\%$) to 9.2 s (at $RH_\infty = 60\%$) when T_∞ was set to 30 °C, whereas it increased from 7.8 s (at $RH_\infty = 30\%$) to 10.6 s (at $RH_\infty = 60\%$) when T_∞ was set to 18 °C. At a constant RH_∞ of 30 % and T_∞ of 18 °C, the calculated lifetime of the droplet decreases from 9.5 s to 7.8 s, while it decreases from 8.6 s to 2.8 s at a constant RH_∞ of 30 % and T_∞ of 30 °C. These results indicate that the effect of RH_∞ on the lifetime of the droplet was higher than that of T_∞ at low RH_∞ values, while

the effect of T_∞ on the lifetime of the droplet was prominent at the low values of RH_∞ and high values of T_∞ . However, a higher T_∞ does not necessarily lead to a decrease in the lifetime of the droplet. The theoretical results were confirmed by the experimental data reported in literatures [31-32]. Morawska et al. [32] reported that the respiratory droplets of the order of 1 μm to 10 μm exist for a few seconds to a few tens of seconds. At the $RH_\infty \leq 40\%$ and $26\text{ °C} \leq T_\infty \leq 30\text{ °C}$, the calculated lifetime of the droplet decreases due to the high evaporation rate. Chen et al. [34] showed that the lifetime of the droplet can decrease at high T_∞ and low RH_∞ values; however, the lifetime of the droplet decreases only for the $RH_\infty < 40\%$. A maximum droplet diameter (29.7 μm) was found at the maximum RH_∞ (60 %) and minimum T_∞ (18 °C), while a minimum droplet diameter (4.9 μm) was found at the minimum RH_∞ (30 %) and maximum T_∞ (30 °C).

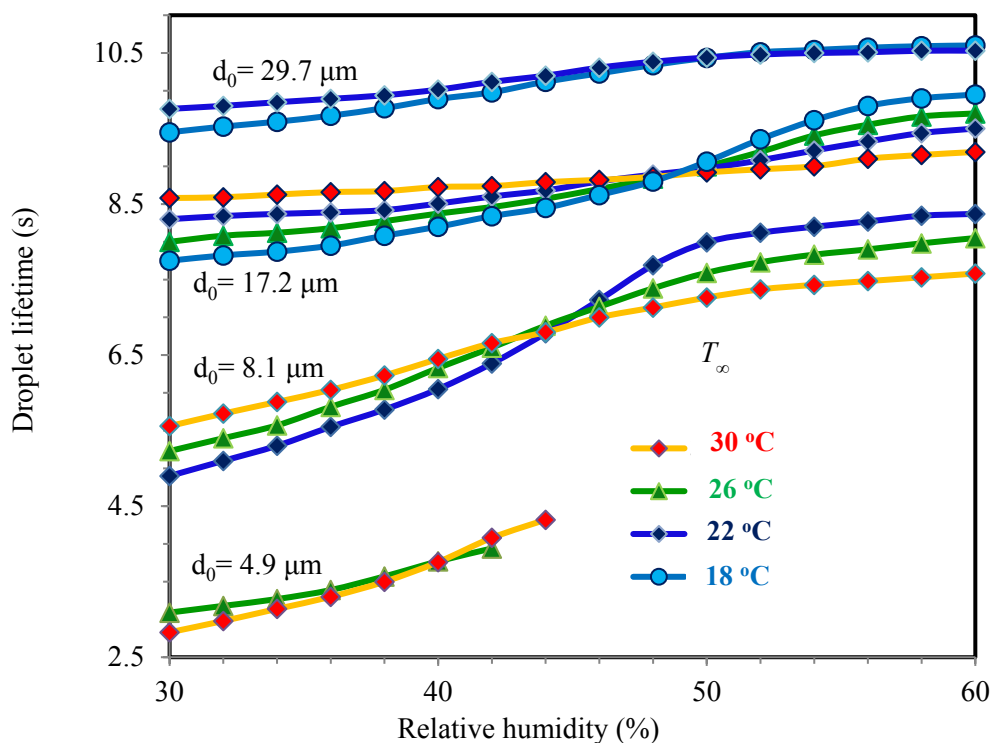


Figure 8. The calculated results of the lifetime of the droplet (t^*) in second (s) versus RH_∞ (%) at different T_∞ values for different initial diameters of the droplet (d_0).

Figure 9 shows the ratio of the lifetime of the droplet with the $T_{\infty} = 30\text{ }^{\circ}\text{C}$ to the lifetime of the droplet with the $T_{\infty} = 18\text{ }^{\circ}\text{C}$ ($t^*_{(30\text{ }^{\circ}\text{C})} / t^*_{(18\text{ }^{\circ}\text{C})}$), which can be obtained from Equation (9). The results show that the ratio of $t^*_{(30\text{ }^{\circ}\text{C})} / t^*_{(18\text{ }^{\circ}\text{C})}$ increased linearly over the RH_{∞} in the range of 30 to 40 %, and considerably increased in the range of 50 to 60 % through a third-order polynomial function. Thus, there is a critical RH_{∞} of 40 %, which is below this value, the lifetime of the droplet is shortened when T_{∞} is set to 30 $^{\circ}\text{C}$ and RH_{∞} is set to 30 %. At the $\text{RH}_{\infty} = 30\%$, the mentioned ratio was 0.78, while its values were 1.0, and 3.85 for the RH_{∞} of 40, and 60 % respectively. The existence of uncertainty in estimating the lifetime of the droplet in the present study can

be attributed to the model assumptions and physical properties of droplets. The effect of T_{∞} on the calculated lifetime of the droplet, due to the assumption of a constant D , will result in an overestimate of the results in the level of 2.1-5.6 %. The deviation of results can be reduced by applying the Chapman-Enskog equation, which represents D as a function of $T^{7/4}$ [36]. In addition, the binary diffusion and constant property assumptions in the droplet phase can be relaxed by the adoption of a multi-component system. Chaudhuri et al. [22] reported that the assumptions including no re-condensation on the droplet surface, and the constant properties of the droplet led to an uncertainty in the estimation of the lifetime of the droplet.

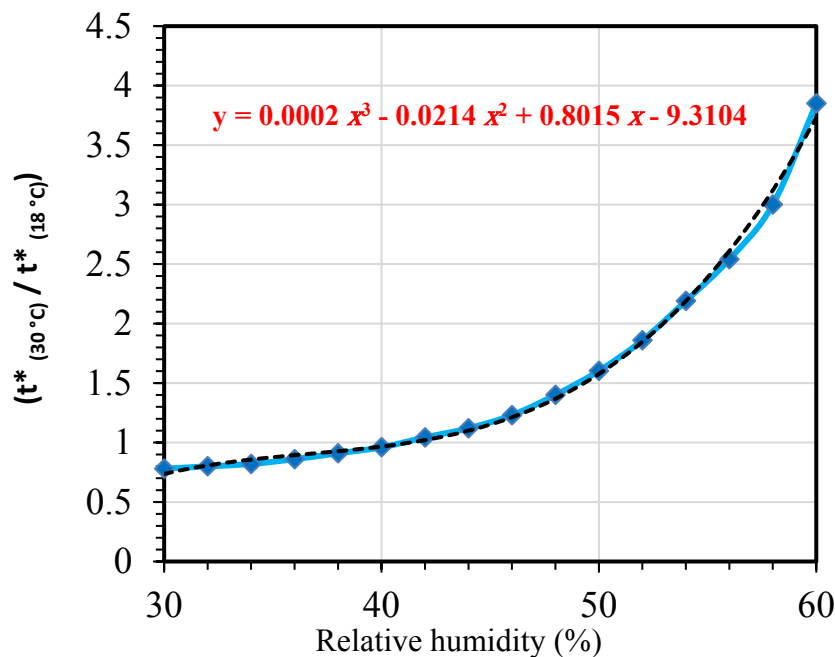


Figure 9. The ratio of the lifetime of the droplet with the $T_{\infty} = 30\text{ }^{\circ}\text{C}$ to the lifetime of the droplet with the $T_{\infty} = 18\text{ }^{\circ}\text{C}$ ($t^*_{(30\text{ }^{\circ}\text{C})} / t^*_{(18\text{ }^{\circ}\text{C})}$).

5. Conclusions

The effect of the indoor temperature (T_{∞}) and relative humidity (RH_{∞}) on the size and lifetime of sneeze droplets with the initial diameters of 4.9, 8.1, 17.2, and 29.7 μm was studied experimentally and theoretically to

elucidate their impacts on the spread of COVID-19. A one-dimensional droplet evaporation model was suggested to calculate the lifetime of the droplet. The main conclusions are as follows:

- (1) The possibility of aerosolized droplet

nuclei being increased from 25.5 to 36.1 % by increasing T_{∞} from 18 to 30 °C and decreased from 36.1 to 13.6 % by reducing RH_{∞} from 60 to 30 %. The effect of the initial diameter of droplets was higher than that of RH_{∞} and also the impact of RH_{∞} was higher than that of T_{∞} on the number of aerosolized droplet nuclei, which represents the final equilibrium diameter of droplets.

(2) The proposed theoretical model showed a significant effect of the initial diameter of the droplet on the lifetime of the droplet over the range of the $26\text{ °C} \leq T_{\infty} \leq 30\text{ °C}$ and $RH_{\infty} \leq 40\%$, while its effect decreased in the range of the $18\text{ °C} \leq T_{\infty} \leq 22\text{ °C}$ and $RH_{\infty} \geq 50\%$, where a minimal shrinkage of droplets took place because of the hygroscopic growth. This finding indicates that a dry and warm environment is suitable for the survival of the virus-containing aerosols to remain airborne.

(3) A critical RH_{∞} of 40 % was found; above them, the lifetime and size distribution of droplets affect RH_{∞} and T_{∞} . At the $RH_{\infty} > 40\%$, the effect of RH_{∞} on the size distribution, and lifetime of droplets was higher than that of T_{∞} . At the $RH_{\infty} < 40\%$, the effect of T_{∞} on the diameter and lifetime of the droplet was higher than that of RH_{∞} . These results indicate that the infection agents controlling strategy were dependent on T_{∞} and RH_{∞} . However, the increase of T_{∞} in the range of 18 to 26 °C and the reduction of RH_{∞} in the range of 30 to 50 % does not necessarily lead to a decrease in the lifetime of the droplet.

(4) It cannot be ignored the effects of the non-volatile content of droplets on the calculation of the lifetime of the droplet. The existence of uncertainty in estimating the lifetime of the droplet in the present

study can be attributed to the assumptions and physical properties of droplets. The results of this study do not imply that the COVID-19 virus will be deactivated at the end of the lifetime of the droplet but represent that controlling the indoor environment is important to the virus-carrying drops.

Acknowledgements

The author would like to thank the Hamedan University of Technology (Grant No. 99/2227) and Iran National Science Foundation (INSF) organization (Grant No. 99022422) for their support.

References

- [1] World Health Organization (WHO), "Modes of transmission of virus causing COVID-19: Implications for IPC precaution recommendations, scientific brief", Geneva, (29 March 2020c). (<https://apps.who.int/iris/handle/10665/331616/>).
- [2] Noorimotlagh, Z., Jaafarzadeh, N. T., Martínez, S. S. and Mirzaee, S. A., "A systematic review of possible airborne transmission of the COVID-19 virus (SARS-CoV-2) in the indoor air environment", *Environ. Res.*, **193** (1), 110612 (2021).
- [3] Huang, C., Wang, Y., Li, X., Ren, L., Zhao, J., Hu, Y., Zhang, L., Fan, G., Xu, J. and Gu, X., "Clinical features of patients infected with 2019 novel coronavirus in Wuhan, China", *Lancet*, **395** (10223), 497 (2020).
- [4] Huang, N., Pérez, P., Kato, T., Mikami, Y., Okuda, K. I., Gilmore, R. C. and Domínguez, C., "The COVID-GRAM tool for patients hospitalized with COVID-19 in Europe", *JAMA Internal*

- Medicine*, **1** (1), 892 (2021).
- [5] Chan, J. F. W., “A familial cluster of pneumonia associated with the 2019 novel coronavirus indicating person-to-person transmission: A study of a family cluster”, *Lancet*, **395** (10223), 514 (2020).
- [6] Liu, J., Liao, X., Qian, S., Yuan, J., Wang, F., Liu, Y., Wang, Z., Wang, F. S., Liu, L. and Zhang, Z., “Community transmission of severe acute respiratory syndrome Coronavirus 2, Shenzhen, China”, *Emerg. Infect. Dis.*, **26** (1), 1320 (2020).
- [7] Balachandar, S., Zaleski, S., Soldati, A., Ahmadi, G. and Bourouiba, L., “Host-to-host airborne transmission as a multiphase flow problem for science-based social distance guidelines”, *Int. J. Multiph. Flow*, **132** (1), 103439 (2020).
- [8] Liu, K., Allahyari, M., Salinas, J. S., Zgheib, N. and Balachandar, S., “Peering inside a cough or sneeze to explain enhanced airborne transmission under dry weather”, *Sci. Rep.*, **11** (1), 9826 (2021).
- [9] Mikszewski, A., Stabile, L., Buonanno, G. and Morawska, L., “Increased close proximity airborne transmission of the SARS-CoV-2 Delta variant”, *Sci. Total Environ.*, **816** (1), 151499 (2022).
- [10] de Oliveira, P. M., Mesquita, L. C. C., Gkantonas, S., Giusti, A. and Mastorakos, E., “Evolution of spray and aerosol from respiratory releases: Theoretical estimates for insight on viral transmission”, *Proc. R. Soc. A*, **477** (2245), 1 (2021).
- [11] Li, H., Leong, F. Y., Xu, G., Ge, Zh., Kang, Ch. W. and Lim, K. H., “Dispersion of evaporating cough droplets in tropical outdoor environment”, *Phys. Fluids*, **32** (1), 113301 (2020).
- [12] Tatsuno, K. and Nagao, S., “Water droplet size measurements in an experimental steam turbine using an optical fiber droplet sizer”, *J. Heat Trans.*, **108** (4), 939 (1986).
- [13] Shang, Y., Tao, Y., Dong, J., He, F. and Tu, J., “Deposition features of inhaled viral droplets may lead to rapid secondary transmission of COVID-19”, *J. Aerosol Sci.*, **154** (1), 105745 (2021).
- [14] Ismail, I. M. I., Rashid, I., Ali, M., Saeed Altaf, B. A. and Munir, M., “Temperature, humidity and outdoor air quality indicators influence COVID-19 spread rate and mortality in major cities of Saudi Arabia”, *Environ. Res.*, **204** (Pt B), 112071 (2022).
- [15] van Doremalen, N., Bushmaker, T., Morris, D. H., Holbrook, M. G., Gamble, A. and Williamson, B. N., “Aerosol and surface stability of SARS-CoV-2 as compared with SARS-Cov-1”, *N. Engl. J. Med.*, **382** (16), 1564 (2020).
- [16] Bourouiba, L., “Turbulent gas clouds and respiratory pathogen emissions: Potential implications for reducing transmission of COVID-19”, *Clinic. Rev. Educ.*, **323** (18), 1837 (2020).
- [17] Bake, B., Larsson, P., Ljungkvist, G., Ljungström, E. and Olin, A., “Exhaled particles and small airways”, *Respiratory Research*, **20** (1), 1 (2019).
- [18] Duguid, J. P., “The size and the duration of air-carriage of respiratory droplets and droplet-nuclei”, *J. Hygiene*, **44** (6), 471 (1946).
- [19] Edwards, D. A., Man, J. C., Brand, P., Katstra, J. P., Sommerer, K., Stone, H. A., Nardell, E. and Scheuch, G., “Inhaling to mitigate exhaled bioaerosols”, *Proc. Natl. Acad. Sci.*, **101** (50), 383 (2004).
- [20] Chao, C., Wan, M., Morawska, L., Johnson, G., Ristovski, Z., Hargreaves, M., Mengersen, K., Corbett, S., Li, Y., Xie, X. and Katoshevski, D.,

- “Characterization of expiration air jets and droplet size distributions immediately at the mouth opening”, *J. Aerosol Sci.*, **40** (2), 122 (2009).
- [21] Han, Z. Y., Weng, W. G. and Huang, Q. Y., “Characterizations of particle size distribution of the droplets exhaled by sneeze”, *J. R. Soc. Interface*, **10** (88), 20130560 (2013).
- [22] Chaudhuri, S., Basu, S., Kabi, P., Unni, V. R. and Saha, A., “Modeling the role of respiratory droplets in Covid-19 type pandemics”, *Phys. Fluids*, **32** (6), 063309 (2020).
- [23] Yin, J., Norviihoho, L. K., Zhou, Zh. F., Chen, B. and Wu, W. T., “Investigation on the evaporation and dispersion of human respiratory droplets with COVID-19 virus”, *Int. J. Multiph. Flow*, **147** (1), 103904 (2022).
- [24] Wang, B., Wu, H. and Wan, X. F., “Transport and fate of human expiratory droplets-A modeling approach”, *Phys. Fluids*, **32** (083307), 1 (2020).
- [25] Rahimi, A. and Bakhshi, A., “A simple one-dimensional model for investigation of heat and mass transfer effects on removal efficiency of particulate matters in a venturi scrubber”, *Iran. J. Chem. Eng. (IChE)*, **6** (4), 3 (2009).
- [26] Robinson, J. F., de Anda, I. R., Moore, F. J., Reid, J. P., Sear, R. P. and Royall, C. P., “Efficacy of face coverings in reducing transmission of COVID-19: Calculations based on models of droplet capture”, *Phys. Fluids*, **33** (1), 1 (2021).
- [27] Liu, L., Wei, J., Li, Y. and Ooi, A., “Evaporation and dispersion of respiratory droplets from coughing”, *Indoor Air*, **27** (1), 179 (2017).
- [28] ANSI/ASHRAE, “ANSI/ASHRAE standard 169-2013”, Climatic data for building design standards, 8400, p. 104 (2013).
- [29] Bahramian, A., Mohammadi, M. and Ahmadi G., “Effect of indoor temperature on the velocity fields and airborne transmission of sneeze droplets: An experimental study and transient CFD modeling”, *Sci. Total Environ.*, **858** (1), 159444 (2023).
- [30] Liu, K., Allahyari, M., Salinas, J. S., Zgheib, N. and Balachandar, S., “Investigation of theoretical scaling laws using large eddy simulations for airborne spreading of viral contagion from sneezing and coughing”, *Phys. Fluids*, **33** (1), 063318 (2021).
- [31] Morawska, L., Johnson, G. R., Ristovski, Z. D., Hargreaves, M., Mengersen, K., Corbett, S., Chao, C. Y. H., Li, Y. and Katoshevski, D., “Size distribution and sites of origin of droplets expelled from the human respiratory tract during expiratory activities”, *J. Aerosol Sci.*, **40** (3), 256 (2009).
- [32] Jafari, S., Khaleghi, H. and Maddahian, R., “Comparative analysis of a single fuel droplet evaporation”, *J. Chem. Petrol. Eng.*, **53** (1), 81 (2019).
- [33] Chen, L. D., “Effect of ambient temperature and humidity on droplet lifetime-A perspective of exhalation sneeze droplets with COVID-19 virus transmission”, *Int. J. Hygiene & Environ. Health*, **229** (1), 113568 (2020).
- [34] Balusamy, S., Banerjee, S. and Sahu, K. C., “Lifetime of sessile saliva droplets in the context of SARS-CoV-2”, *Int. Commun. Heat & Mass Transfer*, **123** (1), 105178 (2021).
- [35] Katre, P., Banerjee, S., Balusamy, S. and Sahu, K. C., “Fluid dynamics of respiratory droplets in the context of

COVID-19: Airborne and surfaceborne transmissions", *Phys. Fluids*, **33** (1), 081302 (2021).

[36] Reid, R. C., Paruznitz, J. M. and Polling,

B. E., *The properties of gases and liquids*, fourth ed., McGraw-Hill, p. 582 (1987).